

Majorana zero modes in quantum Hall edges survive edge reconstruction

Kishore Iyer,¹ Amulya Ratnakar,² Sumathi Rao,³ and Sourin Das²

¹*Aix Marseille Univ, Université de Toulon, CNRS, CPT, Marseille, France*

²*Department of Physics, Indian Institute of Science Education and Research (IISER) Kolkata, Mohanpur - 741246, West Bengal, India*

³*International Centre for Theoretical Sciences, Tata Institute of Fundamental Research, Bengaluru 560089, India*

A smooth edge potential on a $\nu = 1$ quantum Hall system leads to a $\nu = 1/3$ side strip, which could yield both Majorana and parafermion zero modes at the domain wall of the superconductor and ferromagnet on the edge. However, constraints imposed by the $\nu = 1$ bulk allow only for a pair of Majoranas, leading to a $Z_2 \times Z_2$ symmetric ground state. Signatures of both Majoranas appear in the 4π fractional Josephson current when the edge velocities are taken to be different.

PACS numbers:

Introduction:– Non-abelian anyons are particles that possess non-abelian braiding statistics, characterized by degenerate ground states, which can be leveraged to build fault-tolerant qubits¹. Experimental challenges impede the observation of non-abelian anyons in systems such as $\nu = 5/2$ fractional quantum Hall effect (FQHE)^{2,3} and $p + ip$ superconductors⁴, motivating efforts towards engineering non-abelian anyons in heterostructures of conventional materials^{5,6,6}.

Recently, interest has risen in engineering parafermion zero modes (PZM) – Z_N generalization of Majorana zero modes (MZM) – offering richer fault-tolerant qubit operations compared to Majorana-based qubits^{7,8}. Proposals to engineer parafermions involve a pair of FQH edges, proximitized alternatively by superconductors and insulators^{9–17}. Experiments in this direction have observed Crossed-Andreev reflection in graphene as well as 2DEG systems^{18–20}, inspiring focused theoretical investigations in experimentally relevant regimes^{21–30}.

Edge reconstruction, a challenge in interpreting quantum Hall experiments, results from the interplay of electronic correlation in the FQH state and a smooth edge potential^{31–33}. Competition between the need to completely neutralize the positive background and that to form an incompressible droplet leads to the creation of counter-propagating edge modes along the original edge. Edge renormalization refines the edge structure, potentially incorporating upstream neutral modes^{34–37}.

FQH edge experiments aimed at measuring topological properties of the FQHE rely on the bulk-edge correspondence³⁸. While the bulk invariant of the quantum Hall system remains intact under edge reconstruction, it destroys several aspects of the FQH bulk-edge correspondence, with potentially dramatic consequences^{39,40}.

Given the fundamental role of FQH edges in engineering parafermions, it is important to understand the consequences of edge reconstruction on PZM. As a first step, we study MZM built from reconstructed $\nu = 1$ quantum Hall edges, the main focus of this Letter. Edge reconstruction leads to the deposition of a $\nu = 1/3$ FQH side strip along the edge of the $\nu = 1$ QH system, leading ultimately to two upstream bosonic charge modes of conductance $1/3(e^2/h)$ and $2/3(e^2/h)$. The edges of

two such reconstructed $\nu = 1$ QH systems are proximitized with alternating superconductors (SC) and ferromagnets (FM) as shown in Fig. 1. The existence of several bosonic modes on the edge requires adding multiple pairing and backscattering terms to fully gap out the edges. *A priori*, this leads to localized Majorana (due to $\nu = 1$ bulk) and parafermion (due to $\nu = 1/3$ bulk) zero modes on the domain walls between SC and FM. Consistency requirements between the multiple pairing and backscattering terms demote the PZM to an MZM, leading to two decoupled MZMs at each SC-FM domain wall. Hence, despite edge reconstruction, the periodicity of the Josephson current remains 4π though signatures of the multiplicity due to the second Majorana appears in the fractional Josephson current when the propagation velocities of the two charged bosonic modes are different.

Review of $\nu = 1$ edge reconstruction:– In a $\nu = 1$ quantum Hall system, a sharp confining potential yields a single bosonic mode with conductance e^2/h ⁴¹. Smooth edge potentials can create a thin adjacent $\nu = 1/3$ fractional quantum Hall bulk, introducing two counter-propagating edge modes of conductance $1/3$. Edge renormalization, due to interactions and disorder-induced tunneling, results in an edge structure with downstream bosonic modes of conductance $2/3(e^2/h)$ and $1/3(e^2/h)$, and an upstream neutral mode^{34,37}.

The bosonic Hamiltonian density of the reconstructed $\nu = 1$ edge is given by $H_{R/L} = \sum_{\alpha=1}^3 \frac{v_\alpha}{4\pi\nu_\alpha} (\partial_x \phi_{\alpha R/L}(x))^2$, where, ϕ_1 and ϕ_2 denote the bosonic modes with conductance $\nu_1 = 1/3$ and $\nu_2 = 2/3$ respectively. ϕ_3 denotes the neutral mode (of zero conductance) with $\nu_3 = 2$. R/L denotes the chirality and v_α denotes the velocity of ϕ_α . The bosonic fields $\phi_{\alpha R/L}$ obey the commutation relations $[\phi_{\alpha R/L}(x), \phi_{\beta R/L}(y)] = \pm i\pi\nu_\alpha \delta_{\alpha\beta} \text{sgn}(x - y)$.

Given this theory of the reconstructed $\nu = 1$ edge, all possible electron operators on the edge can be calculated⁴². The most relevant electron operators on the considered $\nu = 1$ edge are found to be $\psi_A \sim e^{-i(\phi_1 + \phi_2)}$, $\psi_B \sim e^{-i3\phi_1}$ and $\psi_C \sim e^{-i3/2\phi_2 - i/2\phi_3}$. ψ_A is related to the electron operator on the unreconstructed $\nu = 1$ edge, where the electronic charge is now split into a charge $e/3$ on ϕ_1 and a charge $2e/3$ on ϕ_2 . ψ_B and ψ_C are made up

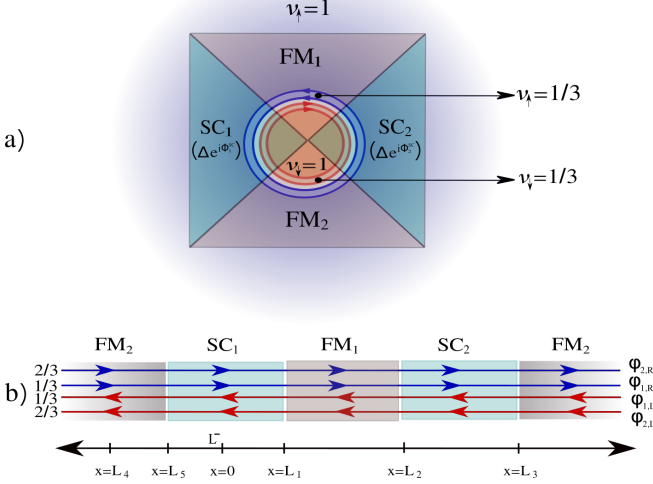


FIG. 1: a) Displays two concentric $\nu_{\uparrow/\downarrow} = 1$ quantum Hall systems, with the inner and outer systems having opposite spins. Edge reconstruction leads to the deposition of thin $\nu_{\uparrow/\downarrow} = 1/3$ FQH bulks along the edges of the $\nu_{\uparrow/\downarrow} = 1$ systems. Their edges are proximitized by alternating superconductors (SC_i) and ferromagnets (FM_i). ϕ_i^{SC} and Δ denote the phase and gap of the SC_i . b) Displays an unfolded version of our setup where the edge physics is transparent. Each reconstructed edge admits two bosonic modes, with an outer mode of conductance of $1/3e^2/h$ ($\phi_{1R/L}$) and an inner mode with conductance of $2/3e^2/h$ ($\phi_{2R/L}$). The neutral mode present in the reconstructed edges is not shown here. R/L denotes the right/left moving bosonic edge modes.

solely of charged excitations on ϕ_1 and, ϕ_2 respectively.

The thin $\nu = 1/3$ bulk is taken to be large enough to accommodate fluxes. Let n be the number of flux quanta in the $\nu = 1$ QH bulk, and m that in the $\nu = 1/3$ FQH side strip. Bulk-edge correspondence dictates that the number of fluxes in the bulk is the same as the charge (quasi-particles) on the edge. The total charge on the reconstructed edge depends on both $\nu = 1$ and $\nu = 1/3$ FQH bulks. A flux quantum in the $\nu = 1$ bulk induces a charge on both $1/3$ (ϕ_1) and $2/3$ (ϕ_2) bosonic modes (corresponding to an ψ_A electron); however, a flux quantum in the $\nu = 1/3$ bulk induces charge only on the $1/3$ (ϕ_1) charge edge mode (three flux quanta correspond to a ψ_B electron). The total charge on ϕ_j , defined as $q_j = 1/2\pi \int dx \partial_x \phi_j$, with $q_1 = \frac{1}{3}(n+m)$ and $q_2 = \frac{2}{3}n$. The total charge on the full edge is $q = q_1 + q_2 = n + m/3$, which in principle can be fractional. We will later see that as the edges are proximitized with superconductors and ferromagnets, energy considerations prevent a total fractional charge on the edges.

Theoretical model:— We now bring together two such edge-reconstructed $\nu = 1$ QH systems with opposite spins. Their edges are proximitized with alternating superconductors (SC) and ferromagnets (FM), as shown in Fig. 1. The system is then described by the bosonized

Hamiltonian, $H = H_0 + H_{SC} + H_{FM}$ where

$$\begin{aligned}
 H_0 &= \sum_{\alpha=1}^2 \frac{\hbar v_{\alpha}}{\nu_{\alpha}} \int dx \left[(\partial_x \varphi_{\alpha}(x))^2 + (\partial_x \theta_{\alpha}(x))^2 \right] \\
 H_{SC} &= - \int dx \{ \Delta_A \cos [2(\varphi_1 + \varphi_2)] + \Delta_B \cos [6\varphi_1] \\
 &\quad + \Delta_C \cos [3\varphi_2] \} \\
 H_{FM} &= - \int dx \{ \mathcal{M}_A \cos [2(\theta_1 + \theta_2)] + \mathcal{M}_B \cos [6\theta_1] \\
 &\quad + \mathcal{M}_C \cos [3\theta_2] \} \quad (1)
 \end{aligned}$$

where ν_{α} denotes the conductance of α^{th} edge, with $\nu_1 = 1/3$, $\nu_2 = 2/3$, and v_{α} denotes the velocity of the α -th bosonic mode. Δ_{γ} and \mathcal{M}_{γ} are the SC and FM pairing amplitudes, having the spatial profile shown in Fig. 1 and $\varphi_{\alpha}/\theta_{\alpha} = (\phi_{\alpha R} \pm \phi_{\alpha L})/2$. The neutral mode, which does not couple to the SC and FM, will be ignored. With the addition of the pairing and backscattering terms in Eq. 1, the edges are fully gapped, and the degeneracy of the ground state can be counted.

Ground-state manifold:— QH regions, whose edges are proximitized by an SC or an FM, can either exchange charge (with the SC) or spin (with the FM). Thus, these regions can be characterized by charge parity (in the SC region) or spin parity (in the FM region) operators. As explained earlier, by bulk-edge correspondence, these charges/spin are the same as the charges/spin at the edges, with them being distributed among the different bosonic modes as

$$\begin{aligned}
 \hat{Q}_i^{(\alpha)} &= \frac{1}{\pi} \int_{SC_i} dx \partial_x \theta_{\alpha}(x) \\
 \hat{S}_i^{(\alpha)} &= \frac{1}{\pi} \int_{FM_i} dx \partial_x \varphi_{\alpha}(x), \quad (2)
 \end{aligned}$$

where $\hat{Q}_i^{(\alpha)}/\hat{S}_i^{(\alpha)}$ is the charge/spin operator defined in the SC_i/FM_i region, with eigenvalues as $q_i^{(\alpha)}/s_i^{(\alpha)}$, where α references the ϕ_{α} boson mode.

We take the limit $\Delta_{\alpha}, \mathcal{M}_{\alpha} \rightarrow \infty$, so that all the cosines in Eq. 1 are pinned to their respective minima. These minima are characterized by integer-valued operators,

$$\begin{aligned}
 (\varphi_1 + \varphi_2)|_{SC_i} &= \pi \hat{N}_i^{\varphi_1 + \varphi_2}; \quad \varphi_2|_{SC_i} = \frac{2\pi}{3} \hat{N}_i^{\varphi_2} \\
 (\theta_1 + \theta_2)|_{FM_i} &= \pi \hat{N}_i^{\theta_1 + \theta_2}; \quad \theta_2|_{FM_i} = \frac{2\pi}{3} \hat{N}_i^{\theta_2} \quad (3)
 \end{aligned}$$

and one can also get $\varphi_1|_{SC_i}$ and $\theta_1|_{SC_i}$ from Eq. 3. \hat{N}_i^{μ} denotes the integer-valued minima to which the field μ is pinned in the i -th SC (for the φ fields) or FM (for the θ fields) regions. They can take values $\hat{N}_i^{\varphi_1 + \varphi_2 / \theta_1 + \theta_2} \in \{0, 1\}$, $\hat{N}_i^{\varphi_1 / \theta_1} \in \{0, \dots, 5\}$ and $\hat{N}_i^{\varphi_2 / \theta_2} \in \{0, 1, 2\}$, where the possible values are dictated by the number of physically distinct minima admitted by the respective cosines.

The operators \hat{N}_i^{μ} and the charge/spin operators defined in Eq. 2 are related by^{26,27}

$$\begin{aligned}
 \hat{Q}_i / \hat{S}_i &= \hat{N}_{i+1}^{\varphi_1 + \varphi_2 / \theta_1 + \theta_2} - \hat{N}_i^{\varphi_1 + \varphi_2 / \theta_1 + \theta_2} \\
 \hat{Q}_i^{(\alpha)} / \hat{S}_i^{(\alpha)} &= \frac{\alpha}{3} \left(\hat{N}_{i+1}^{\theta_{\alpha} / \varphi_{\alpha}} - \hat{N}_i^{\theta_{\alpha} / \varphi_{\alpha}} \right) \quad (4)
 \end{aligned}$$

where $\hat{Q}_i/\hat{S}_i = \sum_{\alpha} \hat{Q}_i^{(\alpha)}/\hat{S}_i^{(\alpha)}$ is the total charge/spin operator for the SC_i/FM_i region. It is then clear that

$$\hat{N}_j^{\varphi_1+\varphi_2/\theta_1+\theta_2} = \text{Mod} \left[\frac{1}{3} \hat{N}_j^{\varphi_1/\theta_1} + \frac{2}{3} \hat{N}_j^{\varphi_2/\theta_2}, 2 \right] \quad (5)$$

that is, only those values of $\hat{N}_j^{\varphi_{\alpha}/\theta_{\alpha}}$ are allowed in the system such that $\hat{N}_j^{\varphi_1+\varphi_2/\theta_1+\theta_2} \in \{0, 1\}$. From Eq. 4 it follows that only integer eigenvalues of \hat{Q}_j/\hat{S}_j are allowed in SC_j/FM_j . That is, despite the existence of a $\nu = 1/3$ bulk, the reconstructed edge always hosts only an integer charge/spin on SC_j/FM_j . Hence, the total charge/spin on the reconstructed edge is also an integer. For non-integer values of charge/spin on SC_j/FM_j , the system moves away from the simultaneous minima of the cosines in Eq. 1.

The charge $e^{i\pi\hat{Q}_i}$ (in SC_i) and spin $e^{i\pi\hat{S}_i}$ (in FM_i) parity operators obey global constraints set by the number of flux quantum in the QH bulks

$$\begin{aligned} \prod_i e^{i\pi\hat{Q}_i} &= e^{i\pi(n_{\uparrow}+n_{\downarrow}+\frac{1}{3}(m_{\uparrow}+m_{\downarrow}))} \\ \prod_i e^{i\pi\hat{S}_i} &= e^{i\pi(n_{\uparrow}-n_{\downarrow}+\frac{1}{3}(m_{\uparrow}-m_{\downarrow}))}, \end{aligned} \quad (6)$$

where $n_{\uparrow/\downarrow}(m_{\uparrow/\downarrow})$ denotes the number of flux quanta in the up/down-spin $\nu_{\uparrow/\downarrow} = 1(1/3)$ bulk. We can now define $q_{totA}/s_{totA} = n_{\uparrow} \pm n_{\downarrow}$ as the total charge/spin in the $\nu = 1$ bulk, and $q_{totB}/s_{totB} = (m_{\uparrow} \pm m_{\downarrow})/3$ as the total charge/spin in the $\nu = 1/3$ bulk. The subscripts A/B remind us that fluxes in the $\nu = 1(1/3)$ bulk, by the bulk-edge correspondence, appear on the edge as $\psi_A(\psi_B)$ electrons, as mentioned earlier. The total charge/spin of the system, denoted by q_{tot}/s_{tot} , is the sum of the total charge/spin on $\nu = 1$ and $1/3$ bulks. By definition, $q_{totA}/s_{totA} \in \{0, 1\}$ since it is the charge in the $\nu = 1$ bulk, and we showed earlier that the total charge/spin on the edge has to be an integer, it follows that $q_{totB}/s_{totB} \in \{0, 1\}$.

The total charge and spin parity of the edges in the SC and FM regions characterize the ground state of the system, and the number of ways these can be distributed in the different SC and FM regions gives the degeneracy of the ground states. From Eq. 6, (q_{totA}, s_{totA}) are constrained to be simultaneously even or odd, and so are (q_{totB}, s_{totB}) , but the two sets are independent of each other. An unreconstructed edge (with no $\nu = 1/3$ side strip) has $q_{totB} = s_{totB} = 0$, giving us 2 distinct parity solutions to the constraints of Eq. 6, consistent with Ref.¹⁰. For a reconstructed system, the number of distinct solutions is doubled compared to an unreconstructed system, since q_{totA} and q_{totB} can be even or odd independently.

The degeneracy of the system, for a fixed q_{totA} and q_{totB} , can be counted by considering the possibilities of distributing the spin parity due to A and B type electrons on the different FM regions. Each state can then be denoted by $|s_{1A}, s_{1B}; s_{2A}, s_{2B}; q_{totA}, q_{totB}\rangle$ with

$$s_{jA} = 3s_j^{(2)}/2; \quad s_{jB} = s_j^{(1)} - s_j^{(2)}/2 \quad (7)$$

$s_{jA/B}$ (defined mod(2)) counts the spin parity due to the A/B type of electrons on the FM_j region. From the allowed values of $s_j^{(\alpha)}$, we can show $s_{jA/B} \in \{0, 1\}$. That is, the spin parity due to each electron can be 0 or 1 in each FM region. This, together with the constraint of Eq. 6 that the total charge and spin due to each electron have to be simultaneously even or odd, leads to 4 degenerate states for a fixed q_{totA} and q_{totB} . Note again that for an unreconstructed edge, the spin and charge due ψ_B electron would be absent, giving back 2 degenerate states for a fixed q_{totA} .

Commutation relations between the charge and spin operators⁷ imply that the action of $e^{i\pi\hat{Q}_i}$ on the ground states transfers a spin due to ψ_A -type electron from FM_i to FM_{i+1} . That is, $e^{i\pi\hat{Q}_1} |s_{1A}, s_{1B}; s_{2A}, s_{2B}; q_{totA}, q_{totB}\rangle = |s_{1A} - 1, s_{1B}; s_{2A} + 1, s_{2B}; q_{totA}, q_{totB}\rangle$. Similarly, the operator $e^{i3\pi\hat{Q}_1^{(1)}}$ transfers a spin due to ψ_B -type electron from FM_i to FM_{i+1} : $e^{3i\pi\hat{Q}_1^{(1)}} |s_{1A}, s_{1B}; s_{2A}, s_{2B}; q_{totA}, q_{totB}\rangle = |s_{1A}, s_{1B} - 1; s_{2A}, s_{2B} + 1; q_{totA}, q_{totB}\rangle$, taking the system between states which cannot be accessed by the action of $e^{i\pi\hat{Q}_i}$. Acting both these operators twice gives back the same state. Hence, the ground state manifold containing 4 states decouples under the action of the operators $e^{i\pi\hat{Q}_i}$ and $e^{3i\pi\hat{Q}_i^{(1)}}$ into 2 disjoint submanifolds containing 2 states each. With the combined action of $e^{i\pi\hat{Q}_i}$ and $e^{i3\pi\hat{Q}_i^{(1)}}$, the system can be rotated into any state in the ground state manifold.

Interface operators:– The doubling of the ground state degeneracy due to the possibility of forming two types of electrons on the edge (ψ_A and ψ_B) implies the existence of two Majorana zero modes at the SC-FM interfaces. The two Majorana operators are denoted by $\chi_{2i-1,\sigma}$ and $\alpha_{2i-1,\sigma}$, at the interface of SC_i and FM_i , and χ_{2i} and α_{2i} at the interface of FM_i and SC_{i+1} , and are given by

$$\begin{aligned} \chi_{2i-1,\sigma} &= e^{i\sigma(\theta_1^{(i)}+\theta_2^{(i)})} \hat{T}_1^C \hat{T}_2^C \prod_{j=1}^i e^{i\pi\hat{S}_{j-1}} \\ \chi_{2i,\sigma} &= e^{i\sigma(\theta_1^{(i)}+\theta_2^{(i)})} \hat{T}_1^C \hat{T}_2^C \prod_{j=1}^i e^{i\pi\hat{S}_j} \\ \alpha_{2i-1,\sigma} &= e^{3i\sigma\theta_1^{(i)}} (\hat{T}_1^C)^3 \prod_{j=1}^i e^{3i\pi\hat{S}_{j-1}^{(1)}} \\ \alpha_{2i,\sigma} &= e^{3i\sigma\theta_1^{(i)}} (\hat{T}_1^C)^3 \prod_{j=1}^i e^{3i\pi\hat{S}_j^{(1)}} \end{aligned} \quad (8)$$

where \hat{T}_1^C and \hat{T}_2^C increase the total charge on the $1/3$ and the $2/3$ bosonic modes by $e/3$ and $2e/3$, respectively. The operator $e^{pi\sigma\theta_{\alpha}^{(i)}}$ adds a spin $p\sigma\nu_{\alpha}$ on FM_i . Since ψ_A and ψ_B cannot transform into each other, reflected in the ground-state manifold being decoupled into two disjoint parts, these two Majoranas are decoupled although they exist at the same physical location. The two decoupled Majoranas can form two distinct resonant levels with their counterparts on opposite interfaces.

Josephson Junction:– Now we take the limit $\mathcal{M}_1 \rightarrow 0$, realizing a Josephson junction between the two SC as shown in Fig. 1. The system is described by the Hamiltonian, $H = H_0 + H_{SC} + H_{FM}$ as given in Eq. 1. The pairing Hamiltonian in the presence of a finite SC

phase bias is given by

$$H_{SC} = - \sum_{\gamma=A,B,C} \Delta_{\gamma} \left(\int_{SC_1} dx \psi_{\gamma} \psi_{\gamma} + \int_{SC_2} dx e^{i\phi_{SC}} \psi_{\gamma} \psi_{\gamma} + hc \right) \quad (9)$$

where the SC phase difference, $\phi_{SC} = \phi_2^{SC} - \phi_1^{SC}$ is plugged into SC_2 using gauge invariance. The above terms translate into cosine operators of the bosonic fields⁷ which in the limit, $\Delta_{\gamma} \rightarrow \infty$, are pinned to their minima, imposing boundary conditions on the bosonic fields in H_0

$$\begin{aligned} (\varphi_1 + \varphi_2)(L_1) &= 0; \varphi_1(L_1) = 0; \varphi_2(L_1) = 0 \\ (\varphi_1 + \varphi_2)(L_2) &= \hat{F}; \varphi_1(L_2) = \hat{F}_1; \varphi_2(L_2) = \hat{F}_2 \end{aligned} \quad (10)$$

$$\begin{aligned} \hat{F} &= \text{mod} \left[\pi \left(\frac{\hat{N}_2^{\varphi_1}}{3} + \frac{2\hat{N}_2^{\varphi_2}}{3} - \frac{\phi_{SC}}{2\pi} \right) + \pi, 2\pi \right] - \pi \\ \hat{F}_2 &= \frac{2}{3} \left(\text{mod} \left[\pi \left(\hat{N}_2^{\varphi_2} - \frac{\phi_{SC}}{2\pi} \right) + \pi, 2\pi \right] - \pi \right) \\ \hat{F}_1 &= \hat{F} - \hat{F}_2 \end{aligned} \quad (11)$$

where the mods are imposed to ensure single-valuedness of the electron operators and spins $s_1^{(1)}$ and $s_1^{(2)}$ to be consistent with the state of the system^{9,26}. The bosonic fields φ_j and θ_j are then mode-expanded to satisfy the boundary conditions and used to diagonalize the Hamiltonian. This gives the low energy part of the Josephson spectrum to be⁷

$$H = \sum_{\alpha=1}^2 \frac{\hbar v_{\alpha} (\hat{\varphi}_{\alpha}(L_2))^2}{2\nu_{\alpha} \pi (L_2 - L_1)}. \quad (12)$$

The energy eigenvalue depends only on the spin parity of different electrons contained in the Josephson junction and is given by $H |s_{1A}, s_{1B}; s_{2A}, s_{2B}; q_{totA}, q_{totB}\rangle = E(s_{1A}, s_{1B}) |s_{1A}, s_{1B}; s_{2A}, s_{2B}; q_{totA}, q_{totB}\rangle$. The Josephson current $J(\phi_{SC})$, is given by $d\langle H \rangle / d\phi_{SC}$, which for $v_1 = v_2$, is sensitive only to the full spin $s_{1A} + s_{1B}$ parity of the junction. Hence, in Fig. 2b there exist overlapping curves corresponding to different spin parities of the different electron types but the same total parities. This feature of the $J_{\phi_{SC}}$ is broken for $v_1 \neq v_2$, where each state distinguished by the spin parity of different electron types has a distinct signature. We show this in Fig. 2d for $v_2/v_1 = 0.5$ where the $J(\phi_{SC})$ in all the different states in the ground-state manifold displays distinct signatures.

Discussion and conclusions:— In this letter, we have studied the effect of edge reconstruction on Majorana zero modes formed on the edges of a $\nu = 1$ quantum Hall system proximitized by superconductors and ferromagnets. Edge reconstruction-induced deposition of an additional $\nu = 1/3$ quantum Hall side strip leads to the possibility of multiple types of electrons existing on the

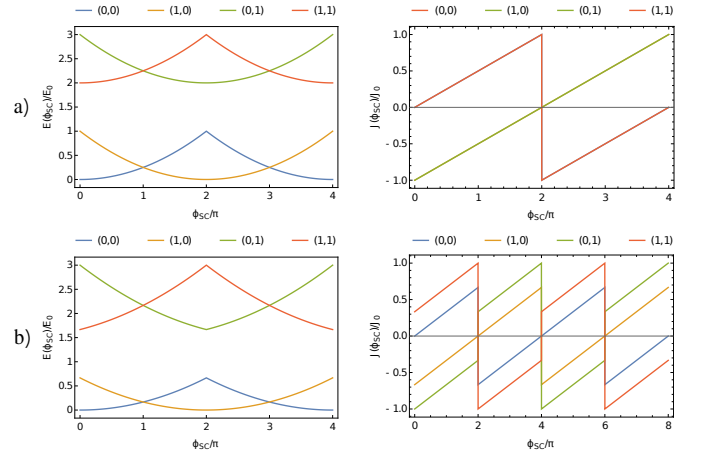


FIG. 2: The energy spectrum ($E(\phi_{SC})$) and the corresponding Josephson current ($J(\phi_{SC})$) is plotted as a function of SC phase bias for different values of (s_{1A}, s_{1B}) . a) shows $E(\phi_{SC})$ and $J(\phi_{SC})$ for equal propagation velocities of the bosonic modes, $v_1 = v_2 = 1$. b) shows $E(\phi_{SC})$ and $J(\phi_{SC})$ when the bosonic modes have different propagation velocities, $v_1 = 0.5v_2 = 1$. The energy eigenvalues ($E(\phi_{SC})$) and Josephson current ($J(\phi_{SC})$) are normalized with respect to the maximum energy (E_0) and Josephson current (J_0) of the $\nu = 1$ unreconstructed edge.

edges. At each SC-FM interface, we find two decoupled Majorana modes that are concerned with the occupancy of two different type of electrons: one related to the $\nu = 1$ bulk excitations, and the other to the $\nu = 1/3$ bulk excitations. It is important to emphasize that the $\nu = 1/3$ bulk does not give rise to a parafermion, but a Majorana as the fractional occupation of the parafermion is energetically unfavorable.

We propose measuring the Josephson current to probe the existence of two decoupled Majoranas at each interface. When the velocities of the $1/3$ and $2/3$ bosonic modes are equal, the fractional Josephson current does not distinguish between the states with the same junction spin parity. When the bosonic mode velocities are different, all the states in the ground-state manifold display distinct signatures in the fractional Josephson current. In all the above scenarios, however, the periodicity of the Josephson current remains 4π with the SC phase bias.

Acknowledgments

A.R. would like to thank Efrat Shimshoni and Ady Stern for useful discussions. A.R. also acknowledges the University Grants Commission, India, for support in the form of a fellowship. S.D. acknowledges the warm hospitality from ICTS during the final stages of writing the draft. K.I. acknowledges support from CEFIPRA through the Raman-Charpak Fellowship, and thanks ICTS for hospitality.

Author contribution:— The first two authors, K.I. and A.R. have contributed equally to this work.

-
- ¹ C. Nayak, S. H. Simon, A. Stern, M. Freedman, and S. Das Sarma, *Rev. Mod. Phys.* **80**, 1083 (2008).
- ² R. Willett, J. P. Eisenstein, H. L. Störmer, D. C. Tsui, A. C. Gossard, and J. H. English, *Phys. Rev. Lett.* **59**, 1776 (1987).
- ³ G. W. Moore and N. Read, *Nucl. Phys. B* **360**, 362 (1991).
- ⁴ A. Y. Kitaev, *Physics-Uspekhi* **44**, 131 (2001).
- ⁵ J. Alicea, *Reports on Progress in Physics* **75**, 076501 (2012).
- ⁶ C. Beenakker, *Annual Review of Condensed Matter Physics* **4**, 113 (2013), <https://doi.org/10.1146/annurev-conmatphys-030212-184337>.
- ⁷ P. Fendley, *Journal of Statistical Mechanics: Theory and Experiment* **2012**, P11020 (2012).
- ⁸ J. Alicea and P. Fendley, *Annual Review of Condensed Matter Physics* **7**, 119 (2016), <https://doi.org/10.1146/annurev-conmatphys-031115-011336>.
- ⁹ D. J. Clarke, J. Alicea, and K. Shtengel, *Nature Communications* **4**, 1348 (2013).
- ¹⁰ N. H. Lindner, E. Berg, G. Refael, and A. Stern, *Phys. Rev. X* **2**, 041002 (2012).
- ¹¹ M. Cheng, *Phys. Rev. B* **86**, 195126 (2012).
- ¹² A. Vaezi, *Phys. Rev. B* **87**, 035132 (2013).
- ¹³ A. Vaezi, *Phys. Rev. X* **4**, 031009 (2014).
- ¹⁴ R. S. K. Mong, D. J. Clarke, J. Alicea, N. H. Lindner, P. Fendley, C. Nayak, Y. Oreg, A. Stern, E. Berg, K. Shtengel, and M. P. A. Fisher, *Phys. Rev. X* **4**, 011036 (2014).
- ¹⁵ U. Khanna, M. Goldstein, and Y. Gefen, *Phys. Rev. B* **105**, L161101 (2022).
- ¹⁶ M. Barkeshli and X.-L. Qi, *Phys. Rev. X* **4**, 041035 (2014).
- ¹⁷ Y. Alavirad, D. Clarke, A. Nag, and J. D. Sau, *Phys. Rev. Lett.* **119**, 217701 (2017).
- ¹⁸ G.-H. Lee, K.-F. Huang, D. K. Efetov, D. S. Wei, S. Hart, T. Taniguchi, K. Watanabe, A. Yacoby, and P. Kim, *Nature Physics* **13**, 693–698 (2017).
- ¹⁹ O. Gül, Y. Ronen, S. Y. Lee, H. Shapourian, J. Zauberman, Y. H. Lee, K. Watanabe, T. Taniguchi, A. Vishwanath, A. Yacoby, and P. Kim, *Phys. Rev. X* **12**, 021057 (2022).
- ²⁰ M. Hatefipour, J. J. Cuzzo, J. Kanter, W. M. Strickland, C. R. Allemang, T.-M. Lu, E. Rossi, and J. Shabani, *Nano Letters* **0**, null (0), pMID: 35867620, <https://doi.org/10.1021/acs.nanolett.2c01413>.
- ²¹ I. E. Nielsen, J. Schulenburg, R. Egger, and M. Burrello, “Dynamics of parafermionic states in transport measurements,” (2023), arXiv:2305.08906 [cond-mat].
- ²² I. E. Nielsen, K. Flensberg, R. Egger, and M. Burrello, *Physical Review Letters* **129**, 037703 (2022).
- ²³ A. B. Michelsen, T. L. Schmidt, and E. G. Idrisov, *Physical Review B* **102**, 125402 (2020).
- ²⁴ N. Schiller, E. Cornfeld, E. Berg, and Y. Oreg, *Physical Review Research* **2**, 023296 (2020).
- ²⁵ N. Schiller, B. A. Katzir, A. Stern, E. Berg, N. H. Lindner, and Y. Oreg, *Physical Review B* **107**, L161105 (2023), publisher: American Physical Society.
- ²⁶ K. Iyer, A. Ratnakar, A. Mukhopadhyay, S. Rao, and S. Das, *Phys. Rev. B* **107**, L121408 (2023).
- ²⁷ K. Snizhko, R. Egger, and Y. Gefen, *Phys. Rev. B* **97**, 081405 (2018).
- ²⁸ Y. Tang, C. Knapp, and J. Alicea, *Physical Review B* **106**, 245411 (2022).
- ²⁹ T. H. Galambos, F. Ronetti, B. Hetényi, D. Loss, and J. Klinovaja, *Phys. Rev. B* **106**, 075410 (2022).
- ³⁰ R. L. R. C. Teixeira, A. Haller, R. Singh, A. Mathew, E. G. Idrisov, L. G. G. V. Dias da Silva, and T. L. Schmidt, *Phys. Rev. Res.* **4**, 043094 (2022).
- ³¹ C. d. C. Chamon and X. G. Wen, *Physical Review B* **49**, 8227 (1994), publisher: American Physical Society.
- ³² X. Wan, E. H. Rezayi, and K. Yang, *Physical Review B* **68**, 125307 (2003).
- ³³ X. Wan, K. Yang, and E. H. Rezayi, *Physical Review Letters* **88**, 056802 (2002).
- ³⁴ C. L. Kane, M. P. A. Fisher, and J. Polchinski, *Phys. Rev. Lett.* **72**, 4129 (1994).
- ³⁵ U. Khanna, M. Goldstein, and Y. Gefen, *Physical Review Letters* **129**, 146801 (2022), publisher: American Physical Society.
- ³⁶ U. Khanna, M. Goldstein, and Y. Gefen, *Low Temperature Physics* **48**, 420 (2022).
- ³⁷ U. Khanna, M. Goldstein, and Y. Gefen, *Physical Review B* **103**, L121302 (2021), publisher: American Physical Society.
- ³⁸ D. Tong, “Lectures on the quantum hall effect,” (2016), arXiv:1606.06687 [hep-th].
- ³⁹ R. Bhattacharyya, M. Banerjee, M. Heiblum, D. Mahalu, and V. Umansky, *Phys. Rev. Lett.* **122**, 246801 (2019).
- ⁴⁰ M. Goldstein and Y. Gefen, *Phys. Rev. Lett.* **117**, 276804 (2016).
- ⁴¹ X. G. Wen, *International Journal of Modern Physics B; (United States)* **6:10** (1992), 10.1142/S0217979292000840.
- ⁴² O. Shtanko, K. Snizhko, and V. Cheianov, *Phys. Rev. B* **89**, 125104 (2014).

Supplemental material for “Majorana zero modes in quantum Hall edges survive edge reconstruction”

I. CHIRAL LUTTINGER LIQUID THEORY OF THE RECONSTRUCTED $\nu = 1$ QUANTUM HALL EDGE

In this section, we describe the chiral Luttinger liquid theory of a reconstructed quantum Hall edge belonging to the $\nu = 1$ bulk. Our starting point is a general edge theory of Abelian quantum Hall systems of filling fraction ν with an arbitrary edge structure, following Ref.⁴². The edge action of a quantum Hall system carrying N bosonic edge modes on the edge is given by

$$S = \frac{1}{4\pi} \int dx dt \sum_{i=1}^N \left(-\chi_i \partial_x \phi_i \partial_t \phi_i - v_i (\partial_x \phi_i)^2 \right) \quad (\text{I.1})$$

where ϕ_i is the bosonic field corresponding to the i^{th} edge mode, v_i denote the propagation velocity of the i^{th} bosonic mode and $\chi_i = \pm 1$ represents the chirality of the i^{th} bosonic mode. The conductance of the i^{th} mode is given by q_i^2 , which must satisfy a constraint determined by the bulk filling factor ν

$$\sum_{i=1}^N \chi_i q_i^2 = \nu. \quad (\text{I.2})$$

The total current and charge density on the edge is given by $\rho(x, t) = \frac{1}{2\pi} \sum_{i=1}^N q_i \partial_x \phi_i(x, t)$ and $J(x, t) = -\frac{1}{2\pi} \sum_{i=1}^N q_i \partial_t \phi_i(x, t)$ respectively, such that the bosonic fields follow the continuity equation $\partial_t \rho(x, t) + \partial_x J(x, t) = 0$. Bosonic field ϕ_i quantized over an edge of length L can be expressed as

$$\phi(x, t) = \hat{\phi}_i^0 + \frac{2\pi}{L} q_i \hat{N}_i X_i + i \sum_{n=1}^{\infty} \sqrt{\frac{2\pi}{Lk}} \left(\hat{a}_{ik} e^{-ikX_i} - \hat{a}_{ik}^\dagger e^{ikX_i} \right) \quad (\text{I.3})$$

where $X_i = -\chi_i x + v_i t$, $k = 2\pi n/L$, $n \in \mathcal{N}$, \hat{a}_{ik} is the bosonic annihilation operator and $\hat{\phi}_i^0$ and \hat{N}_i are the zero mode phase and number operator, with commutation relation $[\hat{a}_{i,k}, \hat{a}_{j,k'}^\dagger] = \delta_{ij} \delta_{kk'}$ and $[\hat{\phi}_i^0, \hat{N}_j] = -i \delta_{ij}$, such that the bosonic fields follows the commutation relation given by $[\phi_i(x, t), \phi_j(x', t')] = -i\pi \text{sgn}(X_i - X'_j) \delta_{ij}$.

A general 1-D electronic field can be represented in terms of bosonic fields as

$$\psi_\alpha(x, t) = \left(\frac{L}{2\pi} \right)^{-\sum_i e_{\alpha,i}^2/2} e^{i \sum_i e_{\alpha,i} \phi_i(x, t)}. \quad (\text{I.4})$$

which satisfy the constraints

$$\begin{aligned} \{\psi_\alpha(x, t), \psi_\alpha(x', t)\} &= 0, \\ \psi_\alpha(x, t) \psi_\beta(x', t) \pm \psi_\beta(x', t), \psi_\alpha(x, t) &= 0, \\ [\rho(x, t), \psi_\alpha(x', t)] &= \delta(x - x') \psi_\alpha(x, t). \end{aligned} \quad (\text{I.5})$$

In terms of the parameters $e_{\alpha,i}$, the constraints are expressed as

$$\begin{aligned} \mathbf{e}_\alpha \cdot \mathbf{e}_\alpha &\in 2\mathbb{Z} + 1, \\ \mathbf{e}_\alpha \cdot \mathbf{e}_\beta &\in \mathbb{Z}, \\ \mathbf{q} \cdot \mathbf{e}_\alpha &= -1, \end{aligned} \quad (\text{I.6})$$

where $\mathbf{e}_\alpha = (e_{\alpha,1}, \dots, e_{\alpha,N})$, $\mathbf{q} = (q_1, \dots, q_N)$ and the operation $\mathbf{A} \cdot \mathbf{B}$ is defined as $\mathbf{A} \cdot \mathbf{B} = \sum_{i=1}^N \chi_i A_i B_i$. The \mathbf{K} matrix for the edge is given by $\mathbf{K}_{\alpha\beta} = \mathbf{e}_\alpha \cdot \mathbf{e}_\beta$.

Now, we use the above formalism to find the electron operators of an edge reconstructed $\nu = 1$ quantum Hall system. Such a system consists of three bosonic modes on its edge: two downstream charged modes with conductance $1/3$ and $2/3$, and a third upstream neutral bosonic mode³⁷. The edge is then described by the charge vector $\mathbf{q} = \left(\sqrt{\frac{1}{3}}, \sqrt{\frac{2}{3}}, 0 \right)$, and the chirality vector $\boldsymbol{\chi} = (1, 1, -1)$. Together with the action of Eq. I.1, these numbers fully describe the edge

theory of the reconstructed $\nu = 1$ system. Solving for \mathbf{e}_α with these inputs of \mathbf{q} and $\boldsymbol{\chi}$, we obtain the following electron operators

$$\begin{aligned}\psi_{A,m}(x,t) &\sim e^{-i\sqrt{\frac{1}{3}}\phi_1 - i\sqrt{\frac{2}{3}}\phi_2 \pm i\sqrt{2m}\phi_3}, \\ \psi_{B,m}(x,t) &\sim e^{-i\sqrt{3}\phi_1 \pm i\sqrt{2-2m}\phi_3}, \\ \psi_{C,m}(x,t) &\sim e^{-i\sqrt{\frac{3}{2}}\phi_2 \pm i\sqrt{\frac{1}{2}-2m}\phi_3}.\end{aligned}\tag{I.7}$$

where m denotes an positive integer. Here, $\psi_{A,m}$ denotes electron fields with composed of excitations on all the three bosonic fields, while $\psi_{B/C,m}$ comprises excitations only on the $\phi_{1/2}$ fields and the neutral mode. In all these classes of electron operators, the ones with the lowest scaling dimension are given by

$$\begin{aligned}\psi_A(x,t) &\sim e^{-i\sqrt{\frac{1}{3}}\phi_1 - i\sqrt{\frac{2}{3}}\phi_2} \\ \psi_B(x,t) &\sim e^{-i\sqrt{3}\phi_1} \\ \psi_C(x,t) &\sim e^{-i\sqrt{\frac{3}{2}}\phi_2 \pm i\sqrt{\frac{1}{2}}\phi_3}.\end{aligned}\tag{I.8}$$

In the main text, we use a notation where the conductances of the bosonic edges appear as coefficients in the action (but not in the definition of charge/current operators.) Then, the commutators of the bosonic fields also gain the conductance as a coefficient to the sign function, becoming: $[\phi_i(x,t), \phi_j(x',t')] = -i\pi\nu_i\delta_{ij}\text{sgn}(X_i - X'_j)$ as given in the main text. In this notation, the electron operators are given by

$$\begin{aligned}\psi_A(x,t) &\propto e^{i\phi_1 + i\phi_2} \\ \psi_B(x,t) &\propto e^{i3\phi_1} \\ \psi_C(x,t) &\propto e^{i\frac{3}{2}\phi_2 \pm i\frac{1}{2}\phi_3}.\end{aligned}\tag{I.9}$$

which is the form of these operators used in the main text.

II. COMMUTATION RELATIONS

Charge on the α -th bosonic mode of SC_1 and SC_2 is given by

$$\begin{aligned}\hat{Q}_1^{(\alpha)} &= \frac{1}{\pi} (\theta_\alpha(x_1) - \theta_\alpha(0) + \theta_\alpha(L) - \theta_\alpha(x_4)) \\ \hat{Q}_2^{(\alpha)} &= \frac{1}{\pi} (\theta_\alpha(x_3) - \theta_\alpha(x_2)),\end{aligned}\tag{II.1}$$

with $\hat{Q}_j = \sum_{\alpha=1,2} \hat{Q}_j^{(\alpha)}$ giving the total charge encompassed in the SC_j region. Similarly, spin content of FM_1 and FM_2 is given by

$$\begin{aligned}\hat{S}_1^{(\alpha)} &= \frac{1}{\pi} (\phi_\alpha(x_2) - \phi_\alpha(x_1)) \\ \hat{S}_2^{(\alpha)} &= \frac{1}{\pi} (\phi_\alpha(x_4) - \phi_\alpha(x_3)).\end{aligned}\tag{II.2}$$

with $\hat{S}_j = \sum_{\alpha=1,2} \hat{S}_j^{(\alpha)}$ being the full spin within FM_j .

The commutation relation of the bosonic fields, $[\phi_\alpha(x), \theta_\beta(y)] = i\pi\nu_\alpha\delta_{\alpha\beta}\Theta(x-y)$, where $\nu_\alpha = \alpha/3, \alpha \in \{1, 2\}$ leads to the following relations for the charge and spin operators

$$\begin{aligned}[\hat{Q}_1^{(\alpha)}, \hat{Q}_2^{(\beta)}] &= [\hat{S}_1^{(\alpha)}, \hat{S}_2^{(\beta)}] = 0 \\ [\hat{Q}_1^{(\alpha)}, \hat{S}_1^{(\beta)}] &= [\hat{Q}_2^{(\alpha)}, \hat{S}_2^{(\beta)}] = -\frac{i\nu_\alpha}{\pi}\delta_{\alpha\beta} \\ [\hat{Q}_2^{(\alpha)}, \hat{S}_1^{(\beta)}] &= [\hat{Q}_1^{(\alpha)}, \hat{S}_2^{(\beta)}] = \frac{i\nu_\alpha}{\pi}\delta_{\alpha\beta}\end{aligned}\tag{II.3}$$

From the above, the commutation relation between the charge and spin parity operators is given by

$$\begin{aligned}[e^{i\pi\hat{Q}_1^{(\alpha)}}, e^{i\pi\hat{Q}_2^{(\beta)}}] &= [e^{i\pi\hat{S}_1^{(\alpha)}}, e^{i\pi\hat{S}_2^{(\beta)}}] = 0 \\ [e^{i\pi\hat{Q}_i^{(\alpha)}}, e^{i\pi\hat{S}_{tot}^{(\beta)}}] &= [e^{i\pi\hat{S}_i^{(\alpha)}}, e^{i\pi\hat{Q}_{tot}^{(\beta)}}] = 0 \\ e^{i\pi\hat{Q}_i^{(\alpha)}} e^{i\pi\hat{S}_j^{(\alpha)}} &= e^{i\pi\nu_\alpha(\delta_{i,j} - \delta_{i+1,j})} e^{i\pi\hat{S}_j^{(\alpha)}} e^{i\pi\hat{Q}_i^{(\alpha)}}\end{aligned}\tag{II.4}$$

where $\hat{S}_{tot}^{(\beta)} = \sum_j \hat{S}_j^{(\beta)}$.

III. BASES FOR THE GROUND STATE MANIFOLD

We consider the system in the limit of $\Delta_\gamma, \mathcal{M}_\gamma$ where all the cosines in Eq. of the main text are pinned to their minima. To label the states in the ground state manifold, it seems natural to diagonalize the Hamiltonian in the basis of the following mutually commuting operators which count the number of fundamental excitations on each bosonic field

$$\left\{ e^{i\pi\hat{S}_1^{(1)}}, e^{i\pi\hat{S}_1^{(2)}}, e^{i\pi\hat{S}_2^{(1)}}, e^{i\pi\hat{S}_2^{(2)}}, e^{i\pi\hat{Q}_{tot}^{(1)}}, e^{i\pi\hat{Q}_{tot}^{(2)}} \right\} \quad (\text{III.1})$$

These operators are characterized by eigenvalues

$$\left\{ e^{i\pi s_1^{(1)}}, e^{i\pi s_1^{(2)}}, e^{i\pi s_2^{(1)}}, e^{i\pi s_2^{(2)}}, e^{i\pi q_{tot}^{(1)}}, e^{i\pi q_{tot}^{(2)}} \right\} \quad (\text{III.2})$$

which allows us to label eigenstates in the ground state manifold as

$$|s_1^{(1)}, s_1^{(2)}; s_2^{(1)}, s_2^{(2)}; q_{tot}^{(1)}, q_{tot}^{(2)}\rangle \quad (\text{III.3})$$

where $s_j^{(1)} \in \{0, 1/3, \dots, 5/3\}$, $s_j^{(2)} \in \{0, 2/3, 4/3\}$. However, to remain on the simultaneous minima of all the pinned cosines, the total spin on each FM region, $s_j^{(1)} + s_j^{(2)} = s_j$ must be an integer. This implies that $s_{tot} = s_{tot}^{(1)} + s_{tot}^{(2)}$ is an integer, and hence, so is $q_{tot} = q_{tot}^{(1)} + q_{tot}^{(2)}$. So, only those combinations of $\{s_1^{(1)}, s_1^{(2)}, s_2^{(1)}, s_2^{(2)}, q_{tot}^{(1)}, q_{tot}^{(2)}\}$ that add up to give integer $\{s_1, s_2, q_{tot}\}$ are allowed within the low energy approximation. The allowed values of the spins and charges are hence: $(s_j^{(1)}, s_j^{(2)}), (q_{tot}^{(1)}, q_{tot}^{(2)}) \in \{(0, 0), (1/3, 2/3), (1, 0), (4/3, 2/3)\}$, such that: $s_1, s_2, q_{tot} \in \{0, 1\}$

The operator $e^{i\pi\hat{Q}_j^{(1)}}$ transfers a spin 1/3 on the one-third bosonic mode from FM_j region to FM_{j+1} and $e^{i\pi\hat{Q}_j^{(2)}}$ transfers a spin 2/3 on the two-third bosonic mode from FM_j region to FM_{j+1} . However, acting these operators individually takes the system out of the ground state manifold. There exist two combinations of these operators that when acted upon a state in the ground state manifold, takes it to yet another state in the manifold. These are: $e^{i\pi\hat{Q}_j^{(1)}} e^{i\pi\hat{Q}_j^{(2)}} = e^{i\pi\hat{Q}_j}$, and $e^{3i\pi\hat{Q}_j^{(1)}}$. The action of these operators on an arbitrary state is as follows

$$\begin{aligned} e^{i\pi\hat{Q}_1} |s_1^{(1)}, s_1^{(2)}; s_2^{(1)}, s_2^{(2)}; q_{tot}^{(1)}, q_{tot}^{(2)}\rangle &= |s_1^{(1)} - 1/3, s_1^{(2)} - 2/3; s_2^{(1)} + 1/3, s_2^{(2)} + 2/3; q_{tot}^{(1)}, q_{tot}^{(2)}\rangle \\ e^{3i\pi\hat{Q}_1^{(1)}} |s_1^{(1)}, s_1^{(2)}; s_2^{(1)}, s_2^{(2)}; q_{tot}^{(1)}, q_{tot}^{(2)}\rangle &= |s_1^{(1)} - 1, s_1^{(2)}; s_2^{(1)} + 1, s_2^{(2)}; q_{tot}^{(1)}, q_{tot}^{(2)}\rangle \end{aligned} \quad (\text{III.4})$$

where $e^{i\pi\hat{Q}_j}$ transfers an electronic spin of the ψ_A -type (composed of one excitation each on the 1/3 and 2/3 bosonic modes) and $e^{3i\pi\hat{Q}_j^{(1)}}$ transfers an electronic spin of the ψ_B -type (composed of three excitations on the 1/3 bosonic mode) from FM_j to FM_{j+1} . The spin operators $e^{i\pi\hat{S}_1^{(1)}}$ and $e^{i\pi\hat{S}_1^{(2)}}$ simply read out the spin on the respective bosonic modes

$$\begin{aligned} e^{i\pi\hat{S}_j^{(1)}} |s_1^{(1)}, s_1^{(2)}; s_2^{(1)}, s_2^{(2)}; q_{tot}\rangle &= e^{i\pi s_j^{(1)}} |s_1^{(1)}, s_1^{(2)}; s_2^{(1)}, s_2^{(2)}; q_{tot}\rangle \\ e^{i\pi\hat{S}_j^{(2)}} |s_1^{(1)}, s_1^{(2)}; s_2^{(1)}, s_2^{(2)}; q_{tot}\rangle &= e^{i\pi s_j^{(2)}} |s_1^{(1)}, s_1^{(2)}; s_2^{(1)}, s_2^{(2)}; q_{tot}\rangle \end{aligned} \quad (\text{III.5})$$

Now we note an ambiguity in the current choice of basis. Assume we are in a state with one ψ_A and one ψ_B type spin on each FM. This state in the current notation is expressed as

$$|4, 1; 4, 1; q_{tot}^{(1)}, q_{tot}^{(2)}\rangle \quad (\text{III.6})$$

Here, the numbers indicate the count of fundamental excitations in the ladder of each bosonic mode. However, given our knowledge of the structure of both electron operators, we can deduce that of the 4 excitations on the 1/3 ladder, 3 come from ψ_B , and 1 comes from ψ_A . The fact that ψ_A has support on both bosonic modes ends up mixing the number of electrons with the numbers of excitations on the bosonic ladders, leading to an ambiguity.

We would like a basis where the numbers of each type of electron, ψ_A and ψ_B , is transparent. For this, we note that ψ_A electrons is always the same as the number of excitations on the 2/3 ladder. One can leverage this information and transform it to a new basis, defined by a different set of mutually commuting set of operators:

$$\left\{ \exp\left(\frac{3i\pi}{2}\hat{S}_1^{(2)}\right), \exp i\pi\left(\hat{S}_1^{(1)} - \frac{\hat{S}_1^{(2)}}{2}\right), \exp\left(\frac{3i\pi}{2}\hat{S}_2^{(2)}\right), \exp i\pi\left(\hat{S}_2^{(1)} - \frac{\hat{S}_2^{(2)}}{2}\right), \exp\left(\frac{3i\pi}{2}\hat{Q}_{tot}^{(1)}\right), \exp i\pi\left(\hat{Q}_{tot}^{(1)} - \frac{\hat{Q}_{tot}^{(2)}}{2}\right) \right\}$$

$\nu = 1$	Sharp edge		Reconstructed edge			
Top. Sec.	q_{totA}		(q_{totA}, q_{totB})			
	0	1	(0, 0)	(1, 1)	(1, 0)	(0, 1)
	0, 0, 0⟩		0, 0, 0, 0, 0, 0⟩	1, 1; 0, 0; 1, 1⟩		
			1, 0; 1, 0; 0, 0⟩	0, 1; 1, 0; 1, 1⟩		
	1, 1, 0⟩		1, 1; 1, 1; 0, 0⟩	0, 0; 1, 1; 1, 1⟩		
			0, 1; 0, 1; 0, 0⟩	1, 0; 0, 1; 1, 1⟩		
		1, 0, 1⟩			1, 0; 0, 0; 1, 0⟩	0, 1; 0, 0; 0, 1⟩
					0, 0; 1, 0; 1, 0⟩	1, 1; 1, 0; 0, 1⟩
		0, 1, 1⟩			1, 1; 0, 1; 1, 0⟩	0, 0; 0, 1; 0, 1⟩
					0, 1; 1, 1; 1, 0⟩	1, 0; 1, 1; 0, 1⟩

TABLE I: The table exhaustively enumerates the ground state manifold of an edge-reconstructed $\nu = 1$ system and contrasts it with that of a sharp or unreconstructed system. The fixed values of total charge parity, called the topological sector (Top. Sec.), for the unreconstructed edge is given by q_{totA} and those for the reconstructed edge are given by (q_{totA}, q_{totB}) . The states in the ground-state manifold are labelled as $|s_{1A}, s_{2A}, q_{totA}\rangle$ for the unreconstructed edge and as $|s_{1A}, s_{1B}; s_{2A}, s_{2B}; q_{totA}, q_{totB}\rangle$ for the reconstructed edge. In a fixed topological sector, the unreconstructed system hosts 2 states, while the edge reconstructed system hosts 4 states. The eigenstates linked by the action of the operator $e^{i\pi\hat{Q}_i}$ are shown in the same colors.

$$\equiv \left\{ e^{i\pi\hat{S}_{1A}}, e^{i\pi\hat{S}_{1B}}, e^{i\pi\hat{S}_{2A}}, e^{i\pi\hat{S}_{2B}}, e^{i\pi\hat{Q}_{totA}}, e^{i\pi\hat{Q}_{totB}} \right\} \quad (\text{III.7})$$

which have the eigenvalues

$$\left\{ e^{\frac{3i\pi}{2}s_1^{(2)}}, e^{i\pi(s_1^{(1)} - s_1^{(2)})/3}, e^{\frac{3i\pi}{2}s_2^{(2)}}, e^{i\pi(s_2^{(1)} - s_2^{(2)})/3}, e^{\frac{3i\pi}{2}q_{tot}^{(2)}}, e^{i\pi(q_{tot}^{(1)} - q_{tot}^{(2)})/3} \right\} \quad (\text{III.8})$$

$$\equiv \left\{ e^{i\pi s_{1A}}, e^{i\pi s_{1B}}, e^{i\pi s_{2A}}, e^{i\pi s_{2B}}, e^{i\pi q_{totA}}, e^{i\pi q_{totB}} \right\}$$

In this basis, by construction, the first entry s_{1A} gives the number of ψ_A -like spin on FM_1 and the second entry s_{1B} gives the number of ψ_B -like spins on FM_1 (and likewise, the third and fourth entries, s_{2A} and s_{2B} for FM_2 .) Similarly, q_{totA} gives the total charge in the system due ψ_A -type electrons and q_{totB} that due to ψ_B -type electrons. The eigenstates are then denoted by the eigenvalues of the above operators

$$|s_{1A}, s_{1B}, s_{1A}, s_{1B}, q_{totA}, q_{totB}\rangle \quad (\text{III.9})$$

which counts explicitly the number of different types of electrons in the system. From the allowed values of s_j^α and $q_{tot}^{(\alpha)}$, we can show the allowed values of spins and charges in the new basis to be $s_{jA/B}, q_{totA/B} \in \{0, 1\}$. We can also show that in the new basis, the charge parity of both types of electrons must be the same as the spin parity of the respective types of electrons. The action of charge operators on these states is as follows

$$e^{i\pi\hat{Q}_1} |s_{1A}, s_{1B}, s_{1A}, s_{1B}, q_{totA}, q_{totB}\rangle = |s_{1A} - 1, s_{1B}, s_{1A} + 1, s_{1B}, q_{totA}, q_{totB}\rangle \quad (\text{III.10})$$

$$e^{3i\pi\hat{Q}_1^{(1)}} |s_{1A}, s_{1B}, s_{1A}, s_{1B}, q_{totA}, q_{totB}\rangle = |s_{1A}, s_{1B} - 1, s_{1A}, s_{1B} + 1, q_{totA}, q_{totB}\rangle$$

where $e^{i\pi\hat{Q}_j}$ transfers a ψ_A -type electronic spin from FM_j to FM_{j+1} , and $e^{3i\pi\hat{Q}_j^{(1)}}$ transfers a ψ_B -type electronic spin from FM_j to FM_{j+1} . These transfers are explicit in the new basis. This is the basis we use to enumerate the ground-state manifold in Table.I.

IV. INTERFACE OPERATORS

We now define physical operators defined at the interface of the SC/FM interface which is analogous to the Majorana operators for $\nu = 1$ (with clean and robust $\nu = 1$ edge) case which will be useful for the topological manipulation in low-energy subspace. We define the operator $\chi_{2i-1,\sigma}$, at the interface of SC_i and FM_i and χ_{2i} at the interface of FM_i and SC_{i+1} (see fig.3), with SC_3 identified as SC_1 . Then,

$$\begin{aligned} \chi_{1\sigma} &= e^{i\sigma(\theta_1^{(1)} + \theta_2^{(1)})} \hat{T}_1^C \hat{T}_2^C \\ \chi_{2\sigma} &= e^{i\sigma(\theta_1^{(1)} + \theta_2^{(1)})} \hat{T}_1^C \hat{T}_2^C e^{i\pi\hat{S}_1} \\ \chi_{3\sigma} &= e^{i\sigma(\theta_1^{(2)} + \theta_2^{(2)})} \hat{T}_1^C \hat{T}_2^C e^{i\pi\hat{S}_1} \\ \chi_{4\sigma} &= e^{i\sigma(\theta_1^{(2)} + \theta_2^{(2)})} \hat{T}_1^C \hat{T}_2^C e^{i\pi\hat{S}_{tot}} \end{aligned} \quad (\text{IV.1})$$

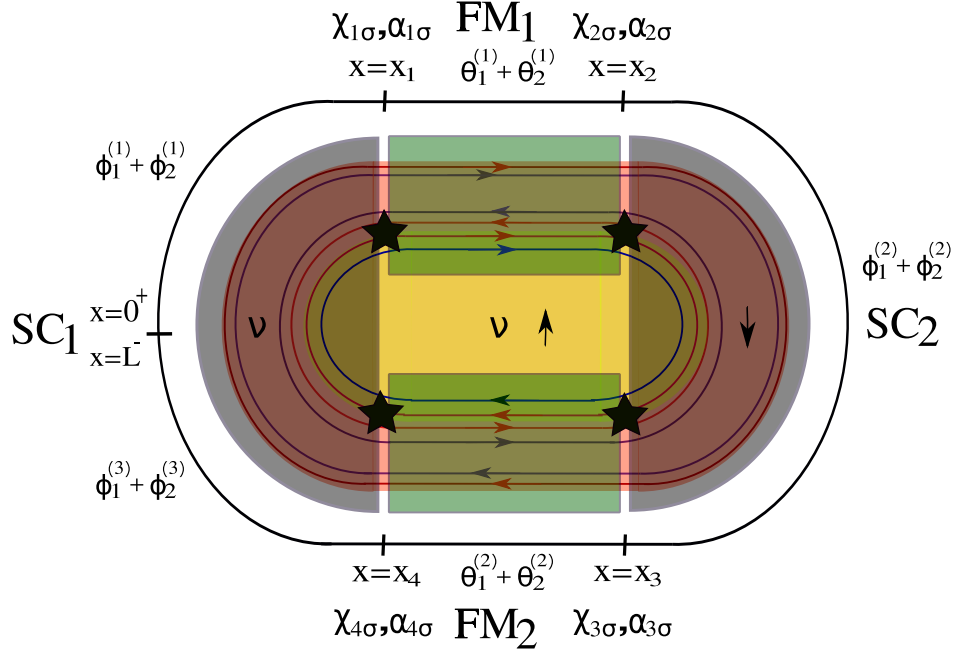


FIG. 3: Schematic shows two quantum Hall systems (shown in light red and light yellow) with different spin (\uparrow and \downarrow) and same filling fraction $\nu = 1$. The boundary of QH systems (of length L) has reconstructed edge states with $1/3$ (in red) and $2/3$ (in blue) conductance. The edge states are gapped out by proximitized superconductors (SC_1 and SC_2) and ferromagnets (FM_1 and FM_2) alternatively. The coordinates are chosen such that the interface between SC and FM are at x_1 , x_2 , x_3 , and x_4 . ϕ_i^j/θ_i^j denotes pinned i^{th} bosonic fields pinned at the j^{th} SC/FM regions, where $i = 1$ and $i = 2$ denotes the $1/3$ and the $2/3$ edge respectively. Zero modes localized at four interfaces are shown by the star. The "Majorana" zero modes, $\chi_{i\sigma}$ and $\alpha_{i\sigma}$ are localized at the interface at x_i .

where $e^{i\sigma(\theta_1^{(i)} + \theta_2^{(i)})}$ adds a spin of σ (consisting of $\sigma/3$ and $(2/3)\sigma$) in the i^{th} FM region, and $\hat{T}_1^C \hat{T}_2^C$ increases the total charge by e (consisting of $e/3$ and $(2/3)e$). As such the operator $\chi_{i\sigma}$ adds a charge and spin of e and σ (of the type $1/3 + 2/3$), respectively. They follow the anti-commutation relation given by $\{\chi_{i\sigma}, \chi_{j\sigma'}\} = 0$ for $i \neq j$. Also, $[\chi_{i\sigma}, \chi_{i,\sigma'}] = 0$.

Similarly, another set of such interface operators could be defined which solely consists of $1/3$ quasi-particles, such that

$$\begin{aligned}
 \alpha_{1\sigma} &= e^{3i\sigma\theta_1^{(1)}} (\hat{T}_1^C)^3 \\
 \alpha_{2\sigma} &= e^{3i\sigma\theta_1^{(1)}} (\hat{T}_1^C)^3 e^{3i\pi\hat{S}_1^{(1)}} \\
 \alpha_{3\sigma} &= e^{3i\sigma\theta_1^{(2)}} (\hat{T}_1^C)^3 e^{3i\pi\hat{S}_1^{(1)}} \\
 \alpha_{4\sigma} &= e^{3i\sigma\theta_1^{(2)}} (\hat{T}_1^C)^3 e^{3i\pi\hat{S}_{tot}^{(1)}},
 \end{aligned} \tag{IV.2}$$

where $S_1^{(1)}$ is the spin content of the $1/3$ edge in the FM_1 region and $S_{tot}^{(1)}$ is $1/3$ edge contribution to the total spin content of the system. Similar to the previous $\chi_{i\sigma}$ operators, $\alpha_{i,\sigma}$ also creates a charge and spin of e and σ (three quasi-particles of $1/3$), respectively. The operators $\alpha_{i\sigma}$ follow the commutation relation given by $\{\alpha_{i\sigma}, \alpha_{j\sigma'}\} = 0$ for $i \neq j$ and $[\alpha_{i\sigma}, \alpha_{i,\sigma'}] = 0$. The commutation relation between $\chi_{i\sigma}$ and $\alpha_{j\sigma'}$ is given by $\{\chi_{i\sigma}, \alpha_{j\sigma'}\} = 0$ for $i \neq j$ and $[\chi_{i\sigma}, \alpha_{i,\sigma'}] = 0$.

The action of operators $\chi_{i\sigma}$ and $\alpha_{i\sigma}$ on the states in the ground state manifold is given by

$$\begin{aligned}
\chi_{1\sigma} |s_{1A}, s_{1B}; s_{2A}, s_{2B}; q_{totA}, q_{totB}\rangle &= e^{i\sigma(\theta_1^{(1)} + \theta_2^{(1)})} \hat{T}_1^C \hat{T}_2^C |s_{1A}, s_{1B}; s_{2A}, s_{2B}; q_{totA}, q_{totB}\rangle \\
&= |s_{1A} + \sigma, s_{1B}; s_{2A}, s_{2B}; q_{totA} + 1, q_{totB}\rangle \\
\chi_{2\sigma} |s_{1A}, s_{1B}; s_{2A}, s_{2B}; q_{totA}, q_{totB}\rangle &= e^{i\sigma(\theta_1^{(1)} + \theta_2^{(1)})} \hat{T}_1^C \hat{T}_2^C e^{i\pi \hat{S}_1} |s_{1A}, s_{1B}; s_{2A}, s_{2B}; q_{totA}, q_{totB}\rangle \\
&= e^{i\pi s_1} |s_{1A} + \sigma, s_{1B}; s_{2A}, s_{2B}; q_{totA} + 1, q_{totB}\rangle \\
\chi_{3\sigma} |s_{1A}, s_{1B}; s_{2A}, s_{2B}; q_{totA}, q_{totB}\rangle &= e^{i\sigma(\theta_1^{(2)} + \theta_2^{(2)})} \hat{T}_1^C \hat{T}_2^C e^{i\pi \hat{S}_1} |s_{1A}, s_{1B}; s_{2A}, s_{2B}; q_{totA}, q_{totB}\rangle \\
&= e^{i\pi s_1} |s_{1A}, s_{1B}; s_{2A} + \sigma, s_{2B}; q_{totA} + 1, q_{totB}\rangle \\
\chi_{4\sigma} |s_{1A}, s_{1B}; s_{2A}, s_{2B}; q_{totA}, q_{totB}\rangle &= e^{i\sigma(\theta_1^{(2)} + \theta_2^{(2)})} \hat{T}_1^C \hat{T}_2^C e^{i\pi \hat{S}_{tot}} |s_{1A}, s_{1B}; s_{2A}, s_{2B}; q_{totA}, q_{totB}\rangle \\
&= e^{i\pi s_{tot}} |s_{1A}, s_{1B}; s_{2A} + \sigma, s_{2B}; q_{totA} + 1, q_{totB}\rangle
\end{aligned} \tag{IV.3}$$

$$\begin{aligned}
\alpha_{1\sigma} |s_{1A}, s_{1B}; s_{2A}, s_{2B}; q_{totA}, q_{totB}\rangle &= e^{3i\sigma\theta_1^{(1)}} (\hat{T}_1^C)^3 |s_{1A}, s_{1B}; s_{2A}, s_{2B}; q_{totA}, q_{totB}\rangle \\
&= |s_{1A}, s_{1B} + \sigma; s_{2A}, s_{2B}; q_{totA}, q_{totB} + 1\rangle \\
\alpha_{2\sigma} |s_{1A}, s_{1B}; s_{2A}, s_{2B}; q_{totA}, q_{totB}\rangle &= e^{3i\sigma\theta_1^{(1)}} (\hat{T}_1^C)^3 e^{3i\pi \hat{S}_1^{(1)}} |s_{1A}, s_{1B}; s_{2A}, s_{2B}; q_{totA}, q_{totB}\rangle \\
&= e^{3i\pi s_1^{(1)}} |s_{1A}, s_{1B} + \sigma; s_{2A}, s_{2B}; q_{totA}, q_{totB} + 1\rangle \\
\alpha_{3\sigma} |s_{1A}, s_{1B}; s_{2A}, s_{2B}; q_{totA}, q_{totB}\rangle &= e^{3i\sigma\theta_1^{(2)}} (\hat{T}_1^C)^3 e^{3i\pi \hat{S}_1^{(1)}} |s_{1A}, s_{1B}; s_{2A}, s_{2B}; q_{totA}, q_{totB}\rangle \\
&= e^{3i\pi s_1^{(1)}} |s_{1A}, s_{1B}; s_{2A}, s_{2B} + \sigma; q_{totA}, q_{totB} + 1\rangle \\
\alpha_{4\sigma} |s_{1A}, s_{1B}; s_{2A}, s_{2B}; q_{totA}, q_{totB}\rangle &= e^{3i\sigma\theta_1^{(2)}} (\hat{T}_1^C)^3 e^{3i\pi \hat{S}_{tot}^{(1)}} |s_{1A}, s_{1B}; s_{2A}, s_{2B}; q_{totA}, q_{totB}\rangle \\
&= e^{3i\pi s_{tot}^{(1)}} |s_{1A}, s_{1B}; s_{2A}, s_{2B} + \sigma; q_{totA}, q_{totB} + 1\rangle
\end{aligned} \tag{IV.4}$$

Also, $\chi_{i\sigma}^2 |s_{1A}, s_{1B}; s_{2A}, s_{2B}; q_{totA}, q_{totB}\rangle = |s_{1A}, s_{1B}; s_{2A}, s_{2B}; q_{totA}, q_{totB}\rangle$ and $\alpha_{i\sigma}^2 |s_{1A}, s_{1B}; s_{2A}, s_{2B}; q_{totA}, q_{totB}\rangle = |s_{1A}, s_{1B}; s_{2A}, s_{2B}; q_{totA}, q_{totB}\rangle$. Hence, $\chi_{i\sigma}$ and $\alpha_{i\sigma}$ operators are the zero modes at the SC-FM interface are the realization of Majorana zero modes in our system.

V. JOSEPHSON JUNCTION

The superconductors on either side of the Josephson junction are modelled by the Hamiltonian

$$H_{SC} = - \sum_{\gamma=A,B,C} \Delta_\gamma \left(\int_{SC_1} dx \psi_\gamma \psi_\gamma + \int_{SC_2} dx e^{i\phi_{SC}} \psi_\gamma \psi_\gamma + hc \right) \tag{V.1}$$

which in the bosonized form reads

$$\begin{aligned}
H_{SC} &= - \int_{SC_1} dx [\Delta_A \cos(2(\phi_1 + \phi_2)) + \Delta_B \cos(6\phi_1) + \Delta_C \cos(3\phi_2)] \\
&\quad - \int_{SC_2} dx [\Delta_A \cos(2(\phi_1 + \phi_2) + \phi_{SC}) + \Delta_B \cos(6\phi_1 + \phi_{SC}) + \Delta_C \cos(3\phi_2 + \phi_{SC})]
\end{aligned} \tag{V.2}$$

where the superconducting phase has been plugged into the second superconductor. In the limit $\Delta_\gamma \rightarrow \infty$, these cosines are all pinned to one of their minima, resulting the in the following boundary conditions of the bosonic fields

$$\begin{aligned}
(\varphi_1 + \varphi_2)(L_1) &= 0; \varphi_1(L_1) = 0; \varphi_2(L_1) = 0 \\
(\varphi_1 + \varphi_2)(L_2) &= \hat{F}; \varphi_1(L_2) = \hat{F}_1; \varphi_2(L_2) = \hat{F}_2
\end{aligned} \tag{V.3}$$

$$\begin{aligned}
\hat{F} &= \text{mod} \left[\pi \left(\frac{\hat{N}_2^{\varphi_1}}{3} + \frac{2\hat{N}_2^{\varphi_2}}{3} - \frac{\phi_{SC}}{2\pi} \right) + \pi, 2\pi \right] - \pi \\
\hat{F}_2 &= \frac{2}{3} \left(\text{mod} \left[\pi \left(\hat{N}_2^{\varphi_2} - \frac{\phi_{SC}}{2\pi} \right) + \pi, 2\pi \right] - \pi \right) \\
\hat{F}_1 &= \hat{F} - \hat{F}_2
\end{aligned} \tag{V.4}$$

where the mods are imposed to ensure single-valuedness of the electron operators, and spins $s_1^{(1)}$ and $s_1^{(2)}$ to be consistent with the state of the system. The effective Hamiltonian of the Josephson junction is given by the free bosonic Hamiltonian

$$H_{\text{eff}} = \sum_{\alpha=1}^2 \frac{\hbar v_{\alpha}}{2\pi\nu_{\alpha}} \int_{L_1}^{L_2} dx \left[(\partial_x \varphi_{\alpha})^2 + (\partial_x \theta_{\alpha})^2 \right] \quad (\text{V.5})$$

where the bosonic fields φ_j and θ_j are subject to the boundary conditions of Eqns. V.3 and V.4. The bosonic field expansion that satisfies these boundary conditions and diagonalizes the Hamiltonian is given by

$$\begin{aligned} \varphi_{\alpha}(x) &= \hat{\varphi}_{\alpha}(L_2) \frac{(x - L_1)}{L_J} + \sqrt{\nu_{\alpha}} \sum_{k=1}^{\infty} i \frac{\sin \lambda_k(x)}{\sqrt{k}} \left(\hat{a}_{\alpha,k} - \hat{a}_{\alpha,k}^{\dagger} \right) \\ \theta_{\alpha}(x) &= \theta_{\alpha}^{(0)} + \sqrt{\nu_{\alpha}} \sum_{k=1}^{\infty} \frac{\cos \lambda_k(x)}{\sqrt{k}} \left(\hat{a}_{\alpha,k} + \hat{a}_{\alpha,k}^{\dagger} \right) \end{aligned} \quad (\text{V.6})$$

where, $\hat{a}_{\alpha,k}$ is the bosonic annihilation operator for the α^{th} bosonic mode, with commutation relations $[\hat{a}_{\alpha,k}, \hat{a}_{\beta,k'}^{\dagger}] = \delta_{kk'} \delta_{\alpha\beta}$, $\lambda_k(x) = \frac{k\pi}{L_J}(x - L_1)$, and $L_J = L_2 - L_1$. $\hat{\varphi}_{\alpha}(L_2)$ and $\theta_{\alpha}^{(0)}$ are zero-mode operators. Correct commutation relations between the φ, θ fields is ensured by imposing $[\hat{N}_2^{\varphi\alpha}, \hat{\theta}_0^{(\alpha)}] = i$. Plugging the field expansion of Eq.V.6, into the effective Hamiltonian

$$H_{\text{eff}} = \sum_{\alpha=1}^2 \hbar v_{\alpha} \left[\frac{(\hat{\varphi}_{\alpha}(L_2))^2}{2\nu_{\alpha}\pi L_J} + \sum_{k=1}^{\infty} \frac{\pi k}{L_J} \left(\hat{a}_{\alpha,k}^{\dagger} \hat{a}_{\alpha,k} + \frac{1}{2} \right) \right] \quad (\text{V.7})$$

from which the Josephson current can be readily obtained as the derivative of the Hamiltonian with respect to the superconducting phase.